Journal of Inflammation Research

Dovepress
open access to scientific and medical research

Open Access Full Text Article

ORIGINAL RESEARCH

RETRACTED ARTICLE: miR-16-5p Regulates Ferroptosis by Targeting SLC7A11 in Adriamycin-Induced Ferroptosis in Cardiomyocytes

Yongquan Chen, Yecheng Deng, Linghua Chen, Ziyao Huang, Yi Yan, Zhaoqi Hua

Department of Cardiology, The Third Affiliated Hospital of Guangzhou Medical University, Guangzhou, People's Republic of Chi

Correspondence: Zhaoqi Huang, Department of Cardiology, The Third Affiliated Hospital of Guangzhou Medical Uni sity, Guan hou, Guangdong, 510150, People's Republic of China, Email zhaoqihuang2007@163.com

Introduction: Adriamycin (ADR) is commonly used in tumor chemotherapy, but it nonreve e cardio icity severely hampers its clinical application. Ferroptosis is an implicated cause of ADR-induced injury. H ver, the unde in molecular mechanisms remain poorly understood. This study explored whether ferroptosis is a pivotal path genic p way underlying ADR-induced cardiotoxicity and the possible molecular mechanisms involved.

Methods: In vivo and in vitro experimental models were used to udy the mechanism o ADR-mediated ferroptosis. Ferroptosis levels were examined in mice and human/rat cardiomyocytes. Mecha istically, the pression levels of SLC7A11 and related miRNAs were examined. Bioinformatics prediction and luciferase reporter ass s were used verify the potential interaction between miR-16-5p and SLC7A11. The biological functions and interaction of SLC7A nd mi 16-5p were investigated in vivo and in vitro.

Results: Our study observed that ADR treatment signifi ntly reased ferroptosis levels in vivo and in vitro. Ferroptosis-related pharmacological interventions further confirmed these resul Our data played that the SLC7A11 level was significantly decreased in cardiac tissues and cells, while an increased e sion lev of miR-16-5p was observed. Moreover, upregulation of SLC7A1 and inhibition of miR-16-5p attenuated ADR-in ced ca iomyoc e ferroptosis injury. Interactive rescue experiments showed that the protective effects of miR-16-5p inhibition ADR d ca iomyocyte injury were blocked by SLC7A11 knockdown.

Discussion: Based on these finding target miR-16-5p could partially reverse the ADR-induced cardiotoxicity by rescuing the SLC7A11 to attenuate ferroptosis his study pr nts a pre-clinical basis to identify miR-16-5p/SLC7A11 as a potential treatment target for ADR-induced cardi xicity

Keywords: adriamycin, c diomyocytes, rroptosis, SLC7A11, miR-16-5p

Introduction

Adriamyc (AD doxo bi) is an anthracycline antibiotic identified as a chemotherapeutic drug since it was first disco d in 19 7. ADR is potent and effective in treating several tumors.[1] However, its clinical utility is restricted by side effec rticularly its irreversible cardiotoxicity and high rate of severe heart failure.[2] A complete understanding of biological me anisms by which ADR exerts its cardiotoxicity has yet to be developed.

Although the underlying molecular mechanisms of ADR-induced cardiomyopathy are multifaceted and have not yet been fully elucidated, they involve oxidative stress, inflammatory response, apoptosis, and mitochondrial dysfunction.[3–5] The recognized mechanism of ADR-induced cardiotoxicity and dysfunction is mainly initiated by reactive oxygen species (ROS). Excessive ROS exceeds the antioxidant defense capacity of myocardial mitochondria, contributing to developing ADR-induced chronic heart failure.[6] When a pathological cardiac injury occurs, iron metabolism in cells is out of balance, and excessive Fe^{2+} presentation leads to an abnormally high level of lipid ROS in cells, so cells are in a state of iron-dependent lipid peroxidation.[7,8] This recently discovered kind of cell death caused by excessive production

Received: 16 October 2022
Accepted: 21 February 2023
Published: 14 March 2023

of Fe^{2+} in cells has been named ferroptosis.[9] It remains unclear mainly whether ferroptosis plays a role in ADR-induced cardiotoxicity and what the molecular mechanisms are.

Various signaling pathways tightly regulate ferroptosis. Researchers have increasingly focused on finding signaling pathways and related genes involved in regulating ferroptosis processes in cardiomyocytes. Solute carrier family 7 member 11 (SLC7A11), a member of the solute carrier family, which encodes xCT, plays a vital role in maintaining redox balance.[10] SLC7A11 transports cystine (entering cells) and glutamate (efferent cells) across the cell membrane in a sodium-independent manner.[11] Reducing cystine to cysteine is the precursor to the biosynthesis of glutathione (GSH), antioxidant protection against lipid peroxidation manufactured by GSH peroxidase 4 (GPX4).

Consequently, by altering the extracellular redox environment, SLC7A11 can affect intracellular signaling pathways and biological functions. Multiple pharmacological agents can modulate ferroptosis activity directly or indirectly through a signaling pathway. Erastin inhibits cystine/glutamate antiporter signaling, accelerating ferroptosis, which is inhibited by iron chelators or ferrostatin-1.[12–14] Until now, little is known about the potential contribution of SLC7A11 shedding to ADR-induced cardiotoxicity.

MicroRNAs (miRNAs) are a class of endogenous, small, single-stranded non-coding RNAs that bind specifically to the 3′ untranslated region of target mRNA.[15] Dysregulation of miRNA is also linked to disease, as miRNA is necessary for normal eukaryotic cell function.[16] Dysregulation of miRNA dysregulation contributes to myocardial injuries.[17] miRNAs are transcribed tissue-specifically and evolutionarily conserved, and their application in clinical practice is promising. Moreover, various miRNAs regulate SLC7A11.[18–20] Whether SLC7A11 contributes to ADR-induced myocardial ferroptosis and its miRNA regulatory mechanism remains unexplored.

Therefore, using in vitro and in vivo studies, this study explored whether ferroptosis is involved in ADR-induced cardiotoxicity, the regulatory mechanism of SLC7A11, and its potential miRNA targets. This study is crucial for further elucidating the possible pathogenesis of ADR-induced cardiotoxicity and the search for potential therapeutic targets.

Materials and Methods

Animal Experiments

Male C57BL/6J mice at the age of 8–10 weeks were obtained from Vital River Laboratories (Beijing, China) and maintained in an environmentally controlled chamber with constant temperature and humidity with a 12-h light/dark cycle with free access to water and food. Animal ethics approval was granted by animal ethics committee of Guangzhou Medical University, and all procedures strictly adhered to the principle of minimizing the animals' pain and suffering. In ADR-induced cardiotoxicity mouse models, ADR was injected intraperitoneally (8 mg/kg) for 4 weeks.[21] Mice were orally treated daily with 75 mg/kg/day of deferiprone (DFP, Santa Cruz Biotechnology) or 10 mg/kg of ferrostatin-1 (Fer-1, Thermo Fisher Scientific) during the administration of ADR.[22,23] Gavaged normal saline was given in the control group for 4 weeks. At the end of experiments, mice were anesthetized with 3% pentobarbital sodium (Sinopec Group Chemical Reagent Co., China). A left ventricular micromanometer catheter of type 1.4-French (Millar Instruments) was inserted, and the left-chamber pressure rise rate (+dp/dt) and left-chamber pressure drop rate (−dp/dt) were recorded. Subsequently, mice were sacrificed, and blood and hearts were collected.

Cell Culture

Cell lines of human cardiomyocytes AC16 and rat cardiomyocytes H9c2 were acquired commercially (Biovector NTCC Inc., Beijing, China) and cultivated in DMEM with 10% fetal bovine serum (FBS) (Gibco, USA) and 1% penicillin-streptomycin in a humid atmosphere at 37 °C and CO2 (5%). During the functional experiments, Erastin (5 μM), Fer-1 (1 μM), or DFP (100 μM) were added correspondingly.

Transfection

Regarding in vitro cell transfection, lentiviral vectors with the sequence of short hairpin RNA (shRNA) targeting SLC7A11 and the control s (SLC7A11-shRNA, SC), miR-16-5p mimic, mimic negative control (miR-NC), miR-16-5p inhibitor and inhibitor NC (miR-NC), pcDNA vector containing SLC7A11 or scramble control, miR-16-5p antagomir

(16-anta) and its scramble control (Scr) were acquired from GenePharma (Shanghai, China). Vectors were transfected into AC16 and H9c2 cells following the instruction book of Lipofectamine™ 3000 Kit (Invitrogen, Carlsbad, CA, USA). For in vivo viral injection, adeno-associated virus (AAV) vectors containing SLC7A11-shRNA, scrabble control vector, or overexpression sequences were developed and obtained from Shanghai GeneChem company (Shanghai, China). Mice were sacrificed 2 weeks after AAV injection, and heart samples were collected.

CCK-8 Assay

The cell was planted in a 96-well plate at a 1 × 103/well cell volume. After treatment and transfection of cells, three replicate wells were established, and cells were placed in the incubator for 24 h and supplemented with 10 μL of CCK-8 solution (Beyotime, Shanghai, China) to each well for 2 h, and the optical density value was determined at λ = 450 nm using the microplate reader (Bio-Rad, Hercules, CA, USA).

Biochemical Analysis

The Fe^{2+} level was tested using an Iron Colorimetric Assay Kit (ScienCell, USA). Additionally, LDH, CK-MB, TBARS, and 4-HNE levels of the cells were analyzed using the corresponding kits purchased from Nanjing Jiangcheng Bioengineering Institute (Nanjing, China). All experimental steps were conducted following the instructions.

Immunofluorescence Assays

For immunofluorescence assays, cardiac sections were fixed with 4% paraformaldehyde. Blocking solution (5% goat serum, 1% bovine serum albumin, and 0.03% Triton X-100) was applied to sections at room temperature for 1 h. Sections were then incubated with the selected primary antibody overnight, and secondary antibodies were selected according to the species of origin of the primary antibodies. Sections were washed with phosphate buffer saline (PBS) three times. DAPI stain (Sigma, Fluoroshield with DAPI) was applied to the nucleus. For measuring intracellular Fe^{2+}, FerroOrange (DojinDo, Japan) was used. Sections cells were visualized under laser scanning confocal microscopy (LSCM) (Leica, Mannheim, Germany).

Western Blotting (WB)

Total proteins were homogenized using radioimmunoprecipitation assay lysis buffer, and the protein concentration was examined using bicinchoninic acid reagent (Sangon Biotech, Shanghai, China). WB was conducted as previously described.[23] Primary antibodies were as follows: rabbit monoclonal antibody Anti-SLC7A11 (PA1-16893, 1:2000, Invitrogen), rabbit monoclonal antibody Anti-GPX4 (ab125066, 1:3000, Abcam), recombinant mouse monoclonal antibody recombinant Anti-Beta-Actin (ab8226, 1:5000, Abcam); Secondary antibodies were IgG H&L horseradish peroxidase labelled (HRP). Beta-Actin antibody was used as the internal reference. Bio-Rad digital Image system was employed to take photos and Image J software (NIH, Bethesda, Maryland, USA) was adopted to analyze the gray values of target bands.

qRT-PCR

Primer sequences were designed for PCR using Primer Premier 5.0 software (PREMIER Biosoft). TRIzol reagent (Beyotime, Shanghai, China) was purchased to extract and purify all RNAs from tissues and cells. Consequently, RNAs were recovered into cDNA using the PrimeScript RT kit (Takara, Dalian, China), and an amplification experiment was performed using the SYBR Premix ExTaqII kit (Takara). Increasing conditions were as follows: 95 °C for 10 min (45 cycles), 95 °C for 15s, 60 °C for 20s, and 72 °C for 20s. Gene expression level was calculated using the $2^{-\Delta\Delta CT}$ method.

Dual-Luciferase Assay

The wild type (WT) or point mutation SLC7A11 promoter sequence (Mut) was synthesized and cloned in pGL3 vector to construct corresponding plasmids. Subsequently, these plasmids were transfected into AC16 and H9c2 cells with corresponding miR-NC, miR-inhibitor, or miR-mimic. After 48 h, the dual-luciferase system (Promega, WI, USA) determined the luciferase activity.

Statistical Analysis

SPSS 21.0 software (IBM Corp. Armonk, NY, USA) and GraphPad Prism 6.0 software (GraphPad Software Inc., San Diego, CA, USA) were used for statistical analyses and plotting. The Shapiro–Wilk test was used for normal distribution detection. Measurement data of normal distribution were depicted as mean ± standard deviation. The *t*-test was used for data comparison between two groups, the one-way analysis of variance (ANOVA) test was used for data comparison among multiple groups, and Tukey's test was used for the post hoc test. *P* was obtained from the bilateral test. Differences were considered of statistical significance at $P < 0.05$.

Results

ADR-Induced Cardiomyocyte Ferroptosis-Related Damage Both in vitro and in vivo

First, the toxicity of chronic ADR was examined in heart tissue. ADR group mice had significantly decreased +dP/dt and -dP/dt than control mice, which confirmed the ADR-induced myocardial injury (Figure 1A–B) ($P < 0.001$). There is an upregulation of LDH and CK-MB in the blood of ADR group mice, indicating the occurrence of myocardial damage (Figure 1C–D) ($P < 0.001$). Measurement of lipid peroxidation in heart tissues was used to determine the TBARS levels, which are correlated with lipid peroxidation. Increased lipid peroxidation levels were observed in ADR group mice (Figure 1E) ($P < 0.001$). Since lipid peroxidation and iron accumulation are ferroptosis features, the iron content and lipid peroxidation of heart tissues were analyzed. Iron ion content was determined using an iron colorimetric assay kit. HNE was the main toxic product of lipid peroxidation and was used to measure lipid peroxidation levels. Heart tissue levels of Fe^{2+} and 4-HNE were further quantified. A significantly higher level of Fe^{2+} and increased 4-HNE content were consistently observed in the heart tissue of ADR group (Figure 1F–G) ($P < 0.001$). Cell phenotypic analysis for the ADR-induced cardiotoxicity cell model was further developed in AC16 cardiomyocytes from human ventricular heart tissues and H9c2 rat myocardial cells. Upon treating cardiomyocytes with ADR, a decrease in cell viability was observed (Figure 1H) ($P < 0.001$). Increased lipid peroxidation detected using a cell-based lipid peroxidation assay kit validated the above results (Figure 1I) ($P < 0.001$). The in vivo data was supported by the in vitro experiment. Treatment with ADR treatment increased the iron and 4-HNE content in the cardiomyocytes H9c2 and AC16 (Figure 1J–K) ($P < 0.001$).

Ferroptosis Contributed Directly to ADR-Induced Cardiotoxicity in vitro and in vivo

Our study further validated the contribution of ferroptosis shedding to ADR cardiotoxicity using Fer-1, a ferroptosis inhibitor, and DFP, an iron chelator. Results found that co-treatment with ADR and Fer-1/DFP significantly ameliorated ADR-induced myocardial injury. Myocardial injury marker levels were significantly decreased in the ADR+Fer-1 and ADR + DFP group, suggesting that Fer-1/DFP alleviates myocardial damage in mice (Figure 2A and B) ($P < 0.01$). In addition, the levels of lipid peroxidation and 4-HNE in the ADR + Fer-1 and ADR + DFP groups were lower than those of ADR group (Figure 2C and D) ($P < 0.01$). Next, the ferroptosis effect on ADR-induced cardiotoxicity was explored in vitro. In in vitro assays, the role of ferroptosis promoter Erastin was further investigated in H9c2 and AC16 cells. Notably, the damage was significantly attenuated with ADR + Fer-1 or ADR+ DFP and an exacerbated effect with ADR + Erastin (Figure 2E) ($P < 0.05$). Coadministration of ADR + Erastin exacerbated ADR-induced ferroptosis of H9c2 and AC16 cells, while ADR + Fer-1 or ADR + DFP decreased it (Figure 2F and G) ($P < 0.01$).

SLC7A11 Mediated ADR-Induced Ferroptosis-Like Cardiotoxicity

Since SLC7A11 plays an essential role in ferroptosis and is linked to ADR-induced chronic cardiotoxicity, SLC7A11-mediated ferroptosis was investigated in vivo and in vitro. In vivo and in vitro, SLC7A11 expression was reduced in ADR-treated cardiomyocytes. The downstream gene, GPX4, showed a similar decrease (Figure 3A) ($P < 0.01$). In vivo, the experimental strategy of SLC7A11 overexpression/knockdown using adenoviral transfection was used to determine the effect of ADR-induced ferroptosis-like cardiotoxicity. WB confirmed the successful SLC7A11 intervention (Figure 3B). Upon ADR administration, SLC7A11 knockdown compromised the CK-MB release in heart tissue, but SLC7A11 overexpression aggravated it (Figure 3B) ($P < 0.01$). Next, H9c2 and AC16 cells were cultured in vitro to

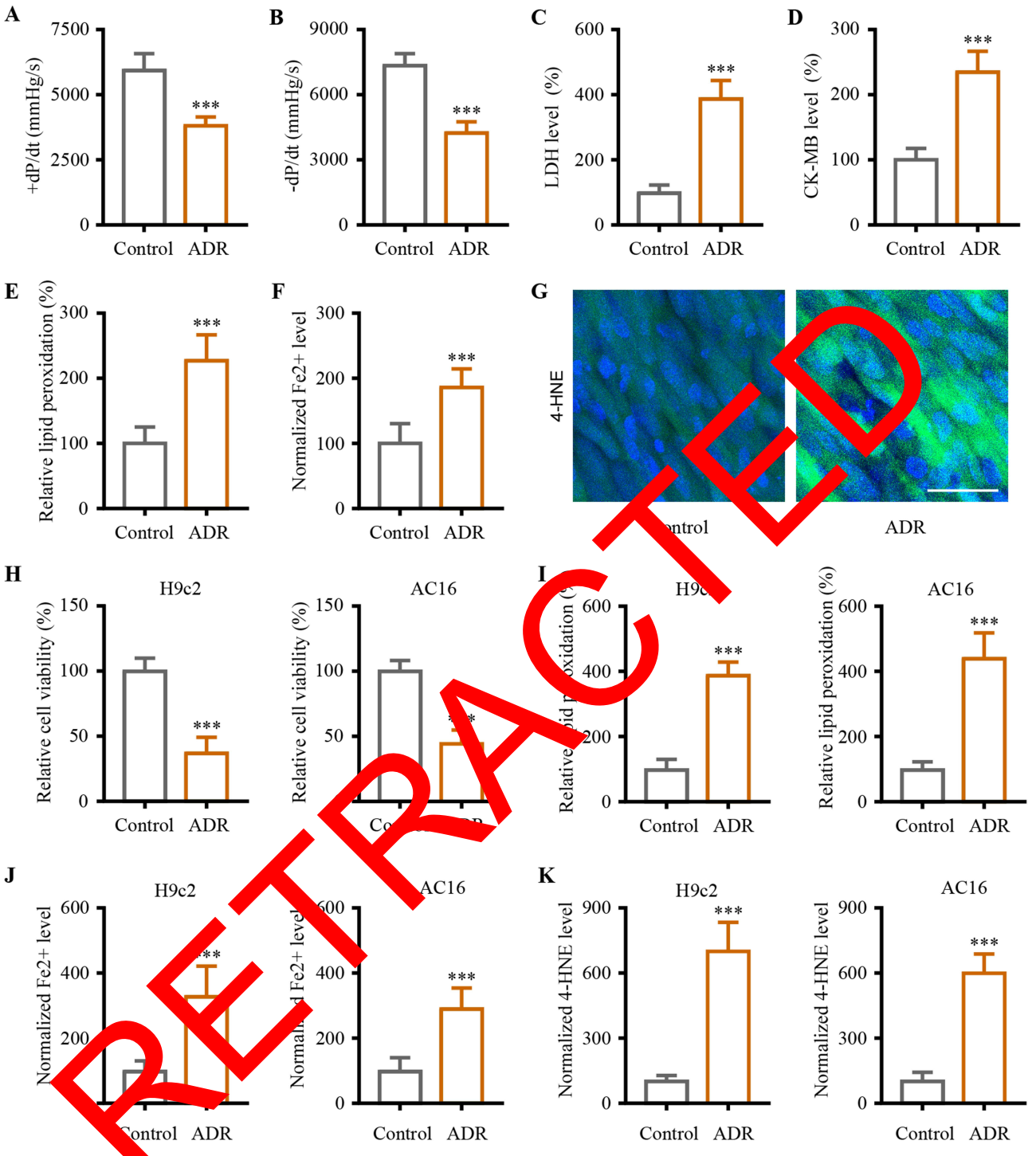

Figure 1 Ferroptosis involved in ADR-induced myocardial injury both in vivo and in vitro. (**A** and **B**) The responses of +dP/dt maximum and -dP/dt maximum in the study groups. (**C** and **D**) ADR-induced myocardial damage were assessed using biochemical cardiotoxicity markers LDH and CK-MB. (**E**) ADR-induced the lipid peroxidation in myocardial tissue. (**F**) We obtained the Fe^{2+} data using iron colorimetric assay. (**G**) The immunofluorescence examination was performed to examine the distribution of 4-HNE. (**H**) Cell viability assays were conducted on H9c2 and AC16 cardiomyocytes in order to evaluate the cytotoxic effects of ADR. (**I**) H9c2 and AC16 cardiomyocytes were measured for lipid peroxidation. (**J**) Levels of Fe^{2+} in the H9c2 and AC16 cells treated with ADR. (**K**) Levels of 4-HNE in the H9c2 and AC16 cells treated with ADR. Data are reported from at least three independent experiments and analysed by independent *t*-test, ***P < 0.001.

determine the effects of SLC7A11 overexpression and knockdown. The results showed that ADR treatment reduced cell viability, while co-transfection of SLC7A11-shRNA significantly exacerbated the cell viability of H9c2 and AC16 cells. On the contrary, ADR-induced cell injury was inhibited in H9c2 and AC16 cells that overexpress SLC7A11 (Figure 2C)

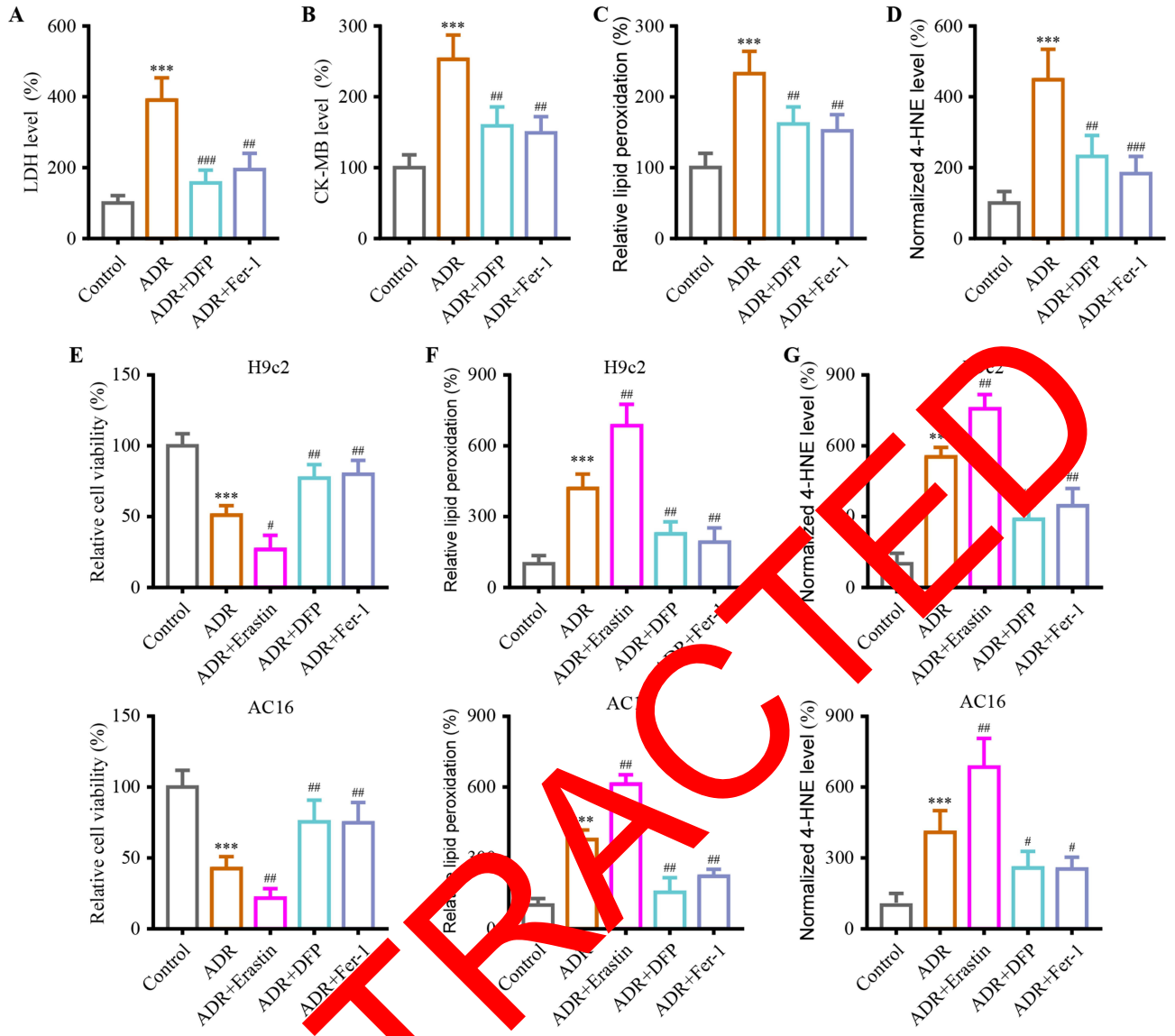

Figure 2 Ferroptosis contribute to ADR-induced myocardial injury mechanism. (**A** and **B**) Co-administration of Fer-1/DFP alleviated ADR-induced myocardial damage assessed using biochemical cardiotoxicity markers LDH and CK-MB in mice. (**C**) Co-administration of Fer-1/DFP decreased ADR-induced the lipid peroxidation in myocardial tissue. (**D**) Co-administration of Fer-1/DFP decreased the expression of 4-HNE in myocardial tissue. (**E**) Cell viability assays were conducted on H9c2 and AC16 cardiomyocytes when co-administration with Erastin/Fer-1/DFP to evaluate the cytotoxic effects of ADR. (**F**) H9c2 and AC16 cardiomyocytes were measured for lipid peroxidation. (**G**) Levels of 4-HNE in H9c2 and AC16 cells were examined when co-administration with Erastin/Fer-1/DFP under ADR. Data are reported from at least three independent experiments and analyzed by one-way ANOVA followed by Dunnett's post hoc test. ***P < 0.001 compared with Control; #P < 0.05, ##P < 0.01, ###P < 0.001 compared with ADR.

($P < 0.01$). Compared to ADR + SC, lipid peroxidation levels were significantly reduced in ADR + SLC7A11-OE (Figure 2D and E) ($P < 0.01$). Conversely, this effect was also present, indicating that SLC7A11 mediated ferroptosis-related lipid peroxidation in H9c2 and AC16 cells.

SLC7A11 is the Direct Target Gene of miR-16-5p

mRNA 3′UTR is targeted by miRNA to modulate gene expression. SLC7A11 targeted miRNA was discovered using the miRNA target prediction program. The potential targets of differentially expressed miRNA were predicted based on miRNA.org and TARGETSCANS miRNA target prediction database (Figure 4A and B). Following ADR administration in mice, miR-16-5p and miR-497-5p were the most significant upregulated candidate prognostic target miRNAs. SLC7A11 expression was negatively associated with miR-16-5p expression in vivo (Figure 4C). The

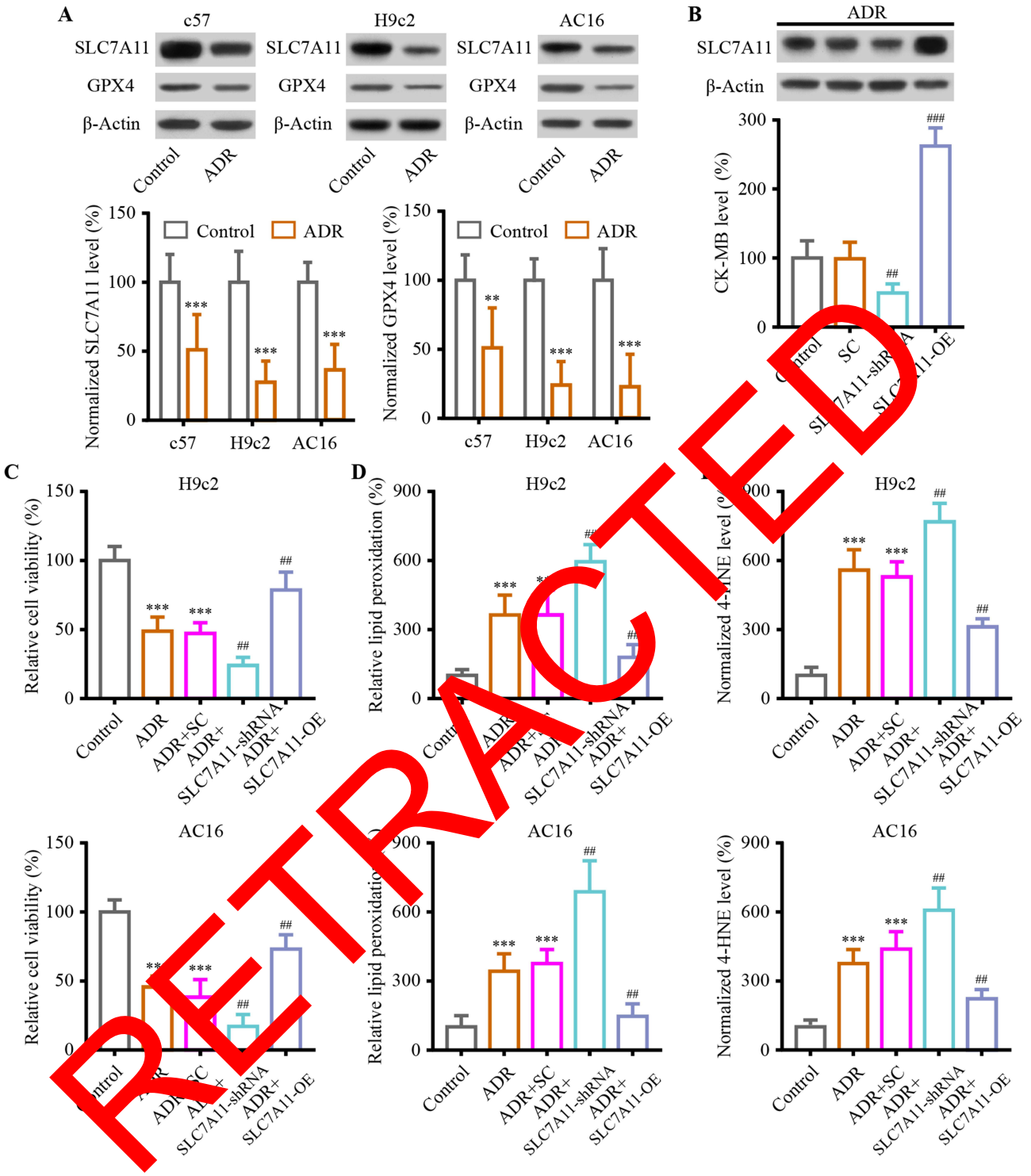

Figure 3 SLC7A11-mediated ferroptosis involved in ADR-induced cardiac injury. (**A**) The ADR induces down-regulation of SLC7A11 and GPX4 expression both in vitro and in vivo. (**B**) The intervention of SLC7A11 mediated ADR-induced cardiac injury assessed using biochemical cardiotoxicity markers CK-MB in mice. (**C**) Cell viability assays were conducted on H9c2 and AC16 cardiomyocytes when SLC7A11 was interfered to mediated ADR-induced cardiac injury. (**D**) H9c2 and AC16 cardiomyocytes were measured for lipid peroxidation. (**E**) Levels of 4-HNE in the H9c2 and AC16 cells were examined when SLC7A11 was interfered under ADR. Data are reported from at least three independent experiments and analysed by one way ANOVA followed by Dunnett's post hoc test. $^{**}P < 0.01$, $^{***}P < 0.001$ compared with Control; $^{\#\#}P < 0.01$, $^{\#\#\#}P < 0.001$ compared with ADR+SC.

results of bioinformatics prediction showed that SLC7A11 could bind to miR-16-5p in several species (Figure 4D). Luciferase reporter displayed that miR-16-5p-mimic declined the luciferase activity of SLC7A11-WT in both H9c2 and AC16 cells but miR-497-5p-mimic failed (Figure 4E). Additionally, the result of the WB assay indicated that

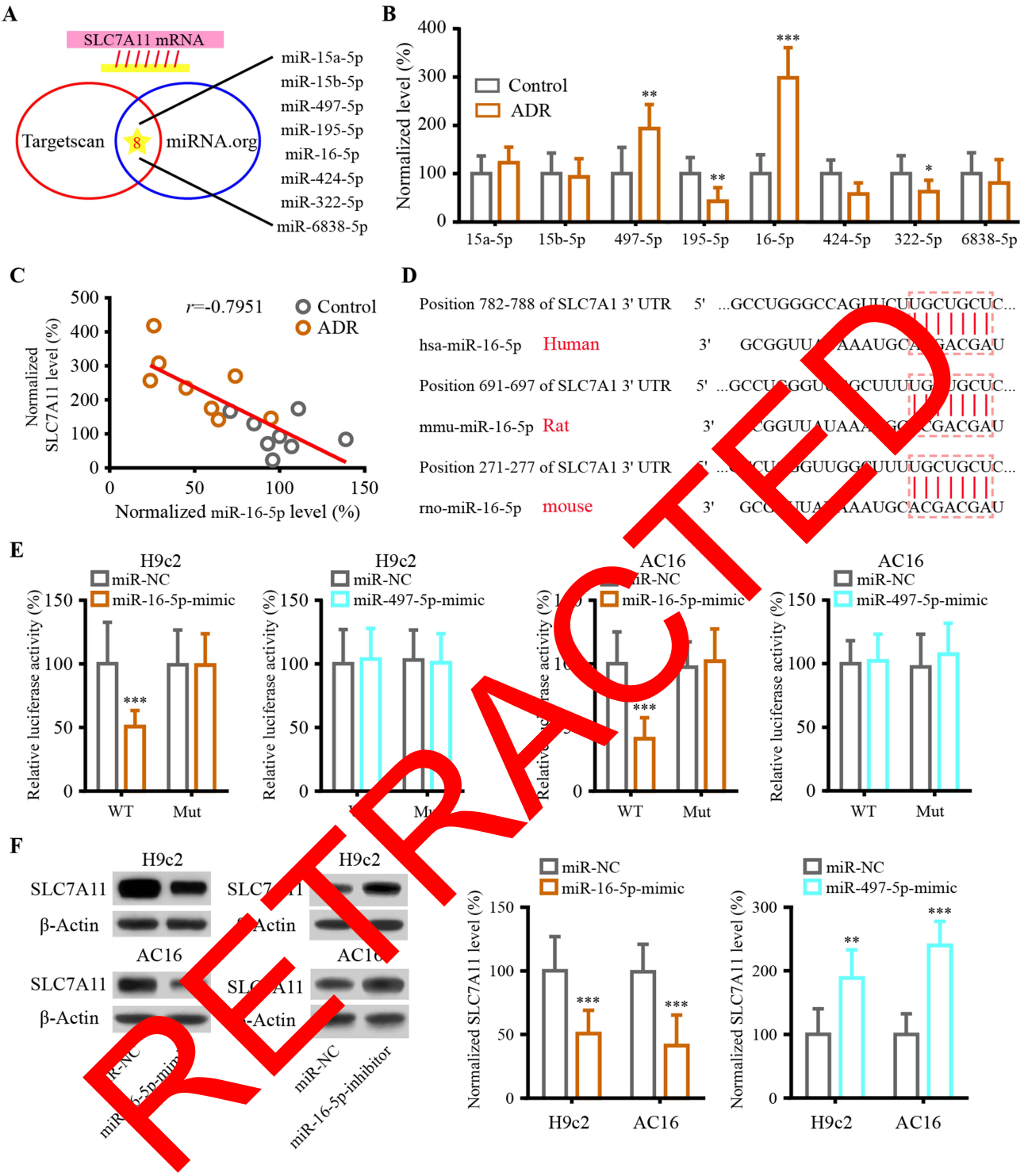

Figure 4 SLC7A11 interacted with miR-16-5p in cardiomyocyte. (**A**) Target prediction programs including miRNA.org and TargetScan were used to identify potential SLC7A11 miRNA targets. (**B**) The expression profiles of SLC7A11's potential target miRNAs. (**C**) Spearman correlation analysis was used to analyze the relationship between the expression of SLC7A11 and miR-16-5p. (**D**) The binding sites between SLC7A11 and miR-16-5p sequences were listed using target prediction tools. (**E**) Following co-transfection of miR-16-5p mimics and wild-type luciferase reporters, the reporter intensity of the mutant reporter was not affected. (**F**) Western blot was used to detect levels of SLC7A11 in H9c2 and AC16 transfected with mimic or inhibitor of miR-16-5p. Data are reported from at least three independent experiments and analysed by independent *t*-test or one way ANOVA followed by Dunnett's post hoc test. *P< 0.05, **P< 0.01, ***P < 0.001 compared with Control; ***P < 0.001 compared with miR-NC.

the decreased SLC7A11 expression was caused by miR-16-5p-mimic transfection. In contrast, SLC7A11 expression was markedly increased by transfection with miR-16-5p-inhibitor. These results showed that miR-16-5p targets SLC7A11.

SLC7A11 Knockdown Neutralized Effect of miR-16-5p in ADR-Induced Cardiac Injury

To analyze the regulatory network of SLC7A11 and miR-16-5p, they were co-transfected into H9c2 and AC16 cells. The transfection of miR-16-5p-inhibitor significantly alleviated the ADR-induced cell viability suppression, while SLC7A11 knockdown blocked the above effect in H9c2 and AC16 cells (Figure 5A). Inhibiting miR-16-5p depleted the lipid peroxidation and 4-HNE levels while downregulating SLC7A11 reversed them (Figure 5B and C). Moreover, AC16 cells were stained with FerroOrange, a dye that reacts specifically with Fe^{2+}. The results determined that signal intensity was significantly reduced after downregulating miR-16-5p, while SLC7A11 knockdown inverted the miR-16-5p-inhibitor roles (Figure 5D). These findings indicated that the down-regulated SLC7A11 inverted the function of miR-16-5p in vitro.

Verification of miR-16-5p/SLC7A11 Axis Function in ADR-Induced Cardiac Injury in vivo

The animal model was further analyzed to confirm the role of miR-16-5p/SLC7A11 axis in vivo. Mice were injected with miR-16-5p antagomir (16-anta) or its scramble control (Scr), SLC7A11-shRNA or Control-shRNA, underwent ADR during the study to explore the pathophysiological role of miR-16-5p/SLC7A11 axis. The WB results revealed that miR-16-5p antagomir efficiently reversed ADR-induced decrease in SLC7A11 expression; meanwhile, lentivirus containing SLC7A11-shRNA made a difference in the reduction in SLC7A11 expression (Figure 6A). Consistently, the administration mentioned above could reverse indexes of heart performance, heart injury, and cardiac lipid peroxidation (Figure 6B–G). The results confirmed that the miR-16-5p/SLC7A11 axis was involved in cardiomyocyte injury under ADR conditions in vivo.

Discussion

The chemotherapeutic drug ADR has been widely used in clinics to treat various types of cancer. However, its use has been limited by toxic effects such as cardiotoxicity. One of the significant challenges is determining how ADR-induced cardiotoxicity is regulated to minimize its caused heart damage. This study established myocardial injury models using ADR in vivo and in vitro and confirmed the involvement and contribution of ferroptosis. These results suggested that SlC7A11/miR-16-5p axis is a new potential therapeutic target in the above pathological changes.

Ferroptosis is a newly discovered form of cell death regulation, usually induced by activating the iron-dependent oxidative stress pathway.[24] Ferroptosis may be involved in organ damage, causing oxidative stress in target organs and tissues and producing many ROS.[25] However, the occurrence and mechanism of ADR-induced ferroptosis in the heart are still largely unknown. Therefore, this study used in vivo and in vitro models to explore the existence and mechanism of ADR-induced ferroptosis contributing to cardiac injury. Our in vivo and in vitro modeling results are consistent with the relevant literature. First, ADR used here successfully induced cardiac injury. In the established model of ADR myocardial injury, the existence of ferroptosis-related molecular markers was successfully detected in both in vivo and in vitro. Our study demonstrated that ferroptosis occurs in ADR-mediated heart injury. With ferroptosis inducer Erastin and ferroptosis inhibitor DFO/Fer-1, all these jointly proved that promoting ferroptosis could enhance, and inhibit ferroptosis could reduce the cardiotoxic effect of ADR. Fer-1 is a lipophilic antioxidant, which mainly plays a role by inhibiting the free radical capture mechanism of lipid peroxidation. The results of fer-1 are consistent with previous studies. Fer-1 can inhibit the occurrence of myocardial injury in ADR-induced mouse models. This further proves that inhibiting ferroptosis can inhibit the progression of ADR-induced myocardial injury. Fer-1 and DFP showed apparent therapeutic and protective effects in vivo experiments, providing a theoretical possibility for clinical application.

SLC7A11 and its downstream GPX4 are essential regulatory genes in ferroptosis,[26] and their reduced expression is a sign of ferroptosis injury. Under normal conditions, SLC7A11/GPX4 can protect cells by consuming the lipid peroxide produced through a series of reactions. However, under certain pathological conditions, the transport capacity of SLC7A11 and the activity of GPX4 decreased, finally inducing ferroptosis.[27] SLC7A11 is expressed in various tissues and downregulated in pathological conditions. Similarly to our results, Li et al[28] recently reported that GPX4 expression decreased in ADR-induced myocardial injury in mice, suggesting that upstream SLC7A11 may participate in the ferroptosis of ADR-induced myocardial injury in mice. Through the direct intervention of SLC7A11, this study

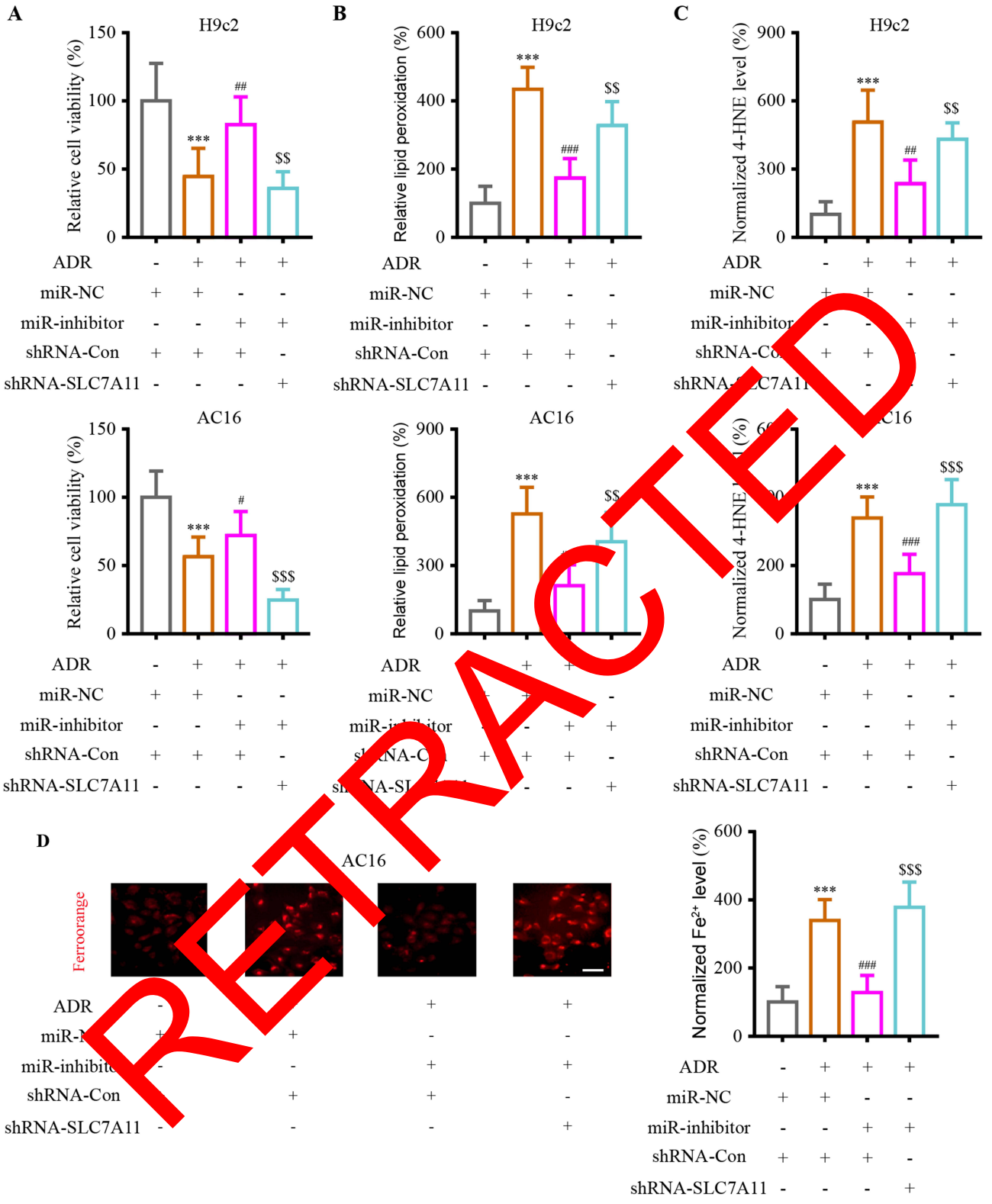

Figure 5 MiR-16-5p functionally interacted with SLC7A11 to reversed the ADR-induced cardiac injury in vitro. (**A**) Analyzing the effect of miR-16-5p/SLC7A11 intervention on cell viability in H9c2 and AC16 cells. (**B**) Analyzing the effect of miR-16-5p/SLC7A11 intervention on lipid peroxidation levels in H9c2 and AC16 cells. (**C**) Analyzing the effect of miR-16-5p/SLC7A11 intervention on lipid peroxidation levels in H9c2 and AC16 cells. (**D**) Analyzing the effect of miR-16-5p/SLC7A11 intervention on Fe^{2+} accumulation in AC16 cells. Data are reported from at least three independent experiments and analysed by independent one way ANOVA followed by Dunnett's post hoc test. ***P < 0.001 compared with miR-NC+shRNA-Con; #P < 0.05, ##P < 0.01, ###P < 0.001 compared with ADR+miR-NC+shRNA-Con; $$P< 0.01, $$$P < 0.001 compared with Control.

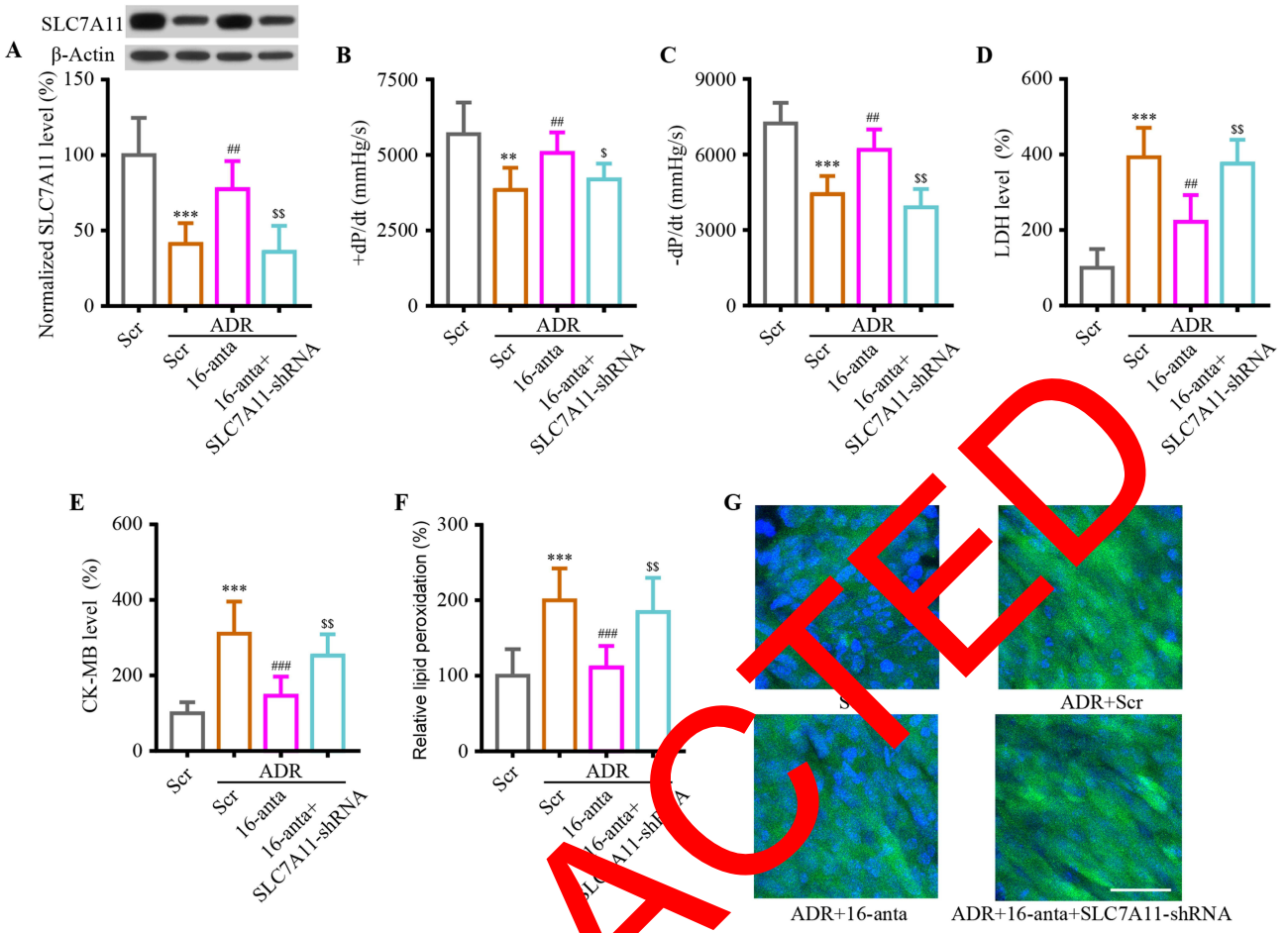

Figure 6 Inhibition of SLC7A11 inverted the effect of miR-16-5p in ADR-induced mice cardiac injury. (**A**) After transfection, Western blotting was performed to detect SLC7A11 expression. (**B** and **C**) After transfection, the heart's performance was examined by performing a +dP/dt and -dP/dt measurement. (**D** and **E**) Total LDH and CK-MB activity in hearts were normalized to total protein content. (**F** and **G**) Both ELISA and immunofluorescence were used to evaluate product of lipid peroxidation. Data are reported from at least three independent experiments and analysed by independent one way ANOVA followed by Dunnett's post hoc test. **P < 0.01, ***P < 0.001 compared with Scr; ##P < 0.01, ###P < 0.001 compared with ADR+Scr; $P< 0.05, $$P < 0.01 compared with ADR+16-anta.

confirmed the direct involvement of SLC7A11 in ADR-induced myocardial injury and ferroptosis in humans, mice, and rat cardiomyocytes. This study found that miR-16-5p had a targeting relationship with SLC7A11, further revealing the regulatory mechanism.

ADR-induced myocardial injury is closely related to abnormal miRNAs expression.[29] Findings on the role of miRNAs in ADR-induced cardiotoxicity have highlighted exploring candidate miRNA as potential diagnostic/therapeutic targets. Typically, miRNAs are complementary to DNA sequences in the 3′UTR of target genes, play a role in post-transcriptional regulation of target gene expression, and participate in various physiological and pathological processes. miR-16-5p is expressed in the heart.[30,31] In other heart injuries, SNHG1/miR165p/GATA4 positive feedback loops protect cardiomyocytes against damage caused by hypoxia/reoxygenation and may provide therapeutic targets for ischemic cardiomyopathy.[32] Consistently, AC16 cells treated with H/R were repressed from apoptosis, diminished LDH and CK-MB activities, and displayed increased viability due to miR-16-5p knockdown.[33] Furthermore, Hayasaka et al[34] demonstrated that miR-16-5p promotes apoptosis in cardiomyocytes via SESN1. This study identified miR-16-5p/SLC7A11 as a potential therapeutic target for ADR-induced cardiotoxicity. The results of in vivo and in vitro validation and the double luciferase reporter gene analysis confirmed a targeted regulatory relationship between miR-16-5p and SLC7A11. Regulating miR-16-5p can significantly interfere with SLC7A11 expression in cardiomyocytes. Concurrently, silencing SLC7A11 alleviated miR-16-5p knockdown-mediated injury in vitro and in vivo.

In animal studies, miRNA agomirs and antagomirs have induced short-term gains or loss of function.[35] Antagomirs were injected into experimental mice to mute their mRNA. The antagomir was injected into the experimental mice to silence miR-16-5p therapeutically. Treatment with MiR-16-5p antagomir before ADR administration markedly improved cardiac function and relieved symptoms of ferroptosis. However, this therapeutic effect was blocked by SLC7A11 knockdown. This study suggests that miR-16-5p-SLC7A11 interactions may be crucial for regulating ADR-induced cardiotoxicity. Our findings indicate that miRNA network-based therapies may effectively treat ADR-induced cardiotoxicity.

Accordingly, this study suggests that cellular ferroptosis plays a crucial role in the pathogenesis of ADR-induced cardiac injury. SLC7A11 overexpression or miR-16-5p knockdown inhibits ferroptosis and exhibits cardioprotective effects in vitro and in vivo. The study revealed a novel regulatory axis involving miR-16-5p/SLC7A11/ferroptosis in ADR-induced cardiotoxicity, which can be used as a potential mechanism for clinical treatment of the heart.

Data Sharing Statement

The datasets used or analysed during the current study are available from the corresponding author on reasonable request.

Ethical Approval

The experiments were approved by the Animal Ethics Committee of Guangzhou Medical University and were performed following the Guide for the Care and Use of Laboratory Animals, published by the National Institutes of Health (NIH Publication No. 85-23, revised 1996).

Author Contributions

All authors made a significant contribution to the work reported, whether that is in the conception, study design, execution, acquisition of data, analysis and interpretation, or in all these areas; took part in drafting, revising or critically reviewing the article; gave final approval of the version to be published; have agreed on the journal to which the article has been submitted; and agree to be accountable for all aspects of the work.

Funding

This study was supported by Special Clinical Technology of Guangzhou (TS20190337).

Disclosure

The authors declare that they have no competing interests in this work.

References

1. Rivankar S. An overview of doxorubicin formulations in cancer therapy. *J Cancer Res Ther*. 2014;10(4):853–858. doi:10.4103/0973-1482.139267
2. Vejpongsa P, Yeh ET. Prevention of anthracycline-induced cardiotoxicity: challenges and opportunities. *J Am Coll Cardiol*. 2014;64(9):938–945. doi:10.1016/j.jacc.2014.06.1167
3. Songbo M, Lang H, Xinyong C, Bin X, Ping Z, Liang S. Oxidative stress injury in doxorubicin-induced cardiotoxicity. *Toxicol Lett*. 2019;307:41–48. doi:10.1016/j.toxlet.2019.02.013
4. Koleini N, Kardami E. Autophagy and mitophagy in the context of doxorubicin-induced cardiotoxicity. *Oncotarget*. 2017;8(28):46663–46680. doi:10.18632/oncotarget.16944
5. Christidi E, Brunham LR. Regulated cell death pathways in doxorubicin-induced cardiotoxicity. *Cell Death Dis*. 2021;12(4):339. doi:10.1038/s41419-021-03614-x
6. He L, Liu F, Li J. Mitochondrial sirtuins and doxorubicin-induced cardiotoxicity. *Cardiovasc Toxicol*. 2021;21(3):179–191. doi:10.1007/s12012-020-09626-x
7. Fang X, Wang H. Ferroptosis as a target for protection against cardiomyopathy. *Proc Natl Acad Sci US A*. 2019;116(7):2672–2680. doi:10.1073/pnas.1821022116
8. Kobayashi M, Suhara T, Baba Y, Kawasaki NK, Higa JK, Matsui T. Pathological roles of iron in cardiovascular disease. *Curr Drug Targets*. 2018;19(9):1068–1076. doi:10.2174/1389450119666180605112235
9. Li J, Cao F, Yin HL, et al. Ferroptosis: past, present and future. *Cell Death Dis*. 2020;11(2):88. doi:10.1038/s41419-020-2298-2
10. Liu X, Olszewski K, Zhang Y. Cystine transporter regulation of pentose phosphate pathway dependency and disulfide stress exposes a targetable metabolic vulnerability in cancer. *Nat Cell Biol*. 2020;22(4):476–486. doi:10.1038/s41556-020-0496-x
11. Koppula P, Zhuang L, Gan B. Cystine transporter SLC7A11/xCT in cancer: ferroptosis, nutrient dependency, and cancer therapy. *Protein Cell*. 2021;12(8):599–620. doi:10.1007/s13238-020-00789-5

12. Li Y, Zeng X, Lu D, Yin M, Shan M, Gao Y. Erastin induces ferroptosis via ferroportin-mediated iron accumulation in endometriosis. *Hum Reprod*. 2021;36(4):951–964. doi:10.1093/humrep/deaa363
13. Miotto G, Rossetto M, Di Paolo ML, et al. Insight into the mechanism of ferroptosis inhibition by ferrostatin-1. *Redox Biol*. 2020;28:101328. doi:10.1016/j.redox.2019.101328
14. Chen X, Yu C, Kang R, Tang D. Iron metabolism in ferroptosis. *Front Cell Dev Biol*. 2020;8:590226. doi:10.3389/fcell.2020.590226
15. Saliminejad K, Khorram Khorshid HR, Soleymani Fard S, Ghaffari SH. An overview of microRNAs: biology, functions, therapeutics, and analysis methods. *J Cell Physiol*. 2019;234(5):5451–5465. doi:10.1002/jcp.27486
16. Carthew RW, Sontheimer EJ. Origins and mechanisms of miRNAs and siRNAs. *Cell*. 2009;136(4):642–655. doi:10.1016/j.cell.2009.01.035
17. Henning RJ. Cardiovascular exosomes and MicroRNAs in cardiovascular physiology and pathophysiology. *J Cardiovasc Transl Res*. 2021;14(2):195–212. doi:10.1007/s12265-020-10040-5
18. Ding C, Ding X, Zheng J, et al. miR-182-5p and miR-378a-3p regulate ferroptosis in I/R-induced renal injury. *Cell Death Dis*. 2020;11(10):929. doi:10.1038/s41419-020-03135-z
19. Lu X, Kang N, Ling X, Pan M, Du W, Gao S. MiR-27a-3p promotes non-small cell lung cancer through SLC7A11-mediated-ferroptosis. *Front Oncol*. 2021;11:759346. doi:10.3389/fonc.2021.759346
20. Wu P, Li C, Ye DM, et al. Circular RNA circEPSTI1 accelerates cervical cancer progression via miR-375/409-3P/[illegible]-SLC7A11 axis. *Aging*. 2021;13(3):4663–4673. doi:10.18632/aging.202518
21. Xiang C, Yan Y, Zhang D. Alleviation of the doxorubicin-induced nephrotoxicity by fasudil in vivo and in vitro. *J Pharmacol Sci*. 2021;145(1):6–15. doi:10.1016/j.jphs.2020.10.002
22. Sripetchwandee J, Khamseekaew J, Svasti S, et al. Deferiprone and efonidipine mitigated iron-overload induced neurotoxicity in wild-type and thalassemic mice. *Life Sci*. 2019;239:116878. doi:10.1016/j.lfs.2019.116878
23. Song D, Zhao L, Li Y, et al. The oral iron chelator deferiprone protects against systemic iron overload-induced retinal degeneration in hepcidin knockout mice. *Invest Ophthalmol Vis Sci*. 2014;55(7):4525–4532. doi:10.1167/iovs.14-14568
24. Hong M, Rong J, Tao X, Xu Y. The emerging role of ferroptosis in cardiovascular diseases. *Front Pharmacol*. 2022;13:822083. doi:10.3389/fphar.2022.822083
25. Huang J, Wu R, Chen L, Yang Z, Yan D, Li M. Understanding anthracycline cardiotoxicity from the mitochondrial aspect. *Front Pharmacol*. 2022;13:811406. doi:10.3389/fphar.2022.811406
26. Zhao MY, Liu P, Sun C, Pei LJ, Huang YG. Propofol augments paclitaxel-induced cervical cancer cell ferroptosis in vitro. *Front Pharmacol*. 2022;13:816432. doi:10.3389/fphar.2022.816432
27. Liu J, Zhang M, Qin C, et al. Resveratrol attenuate myocardial injury by inhibiting ferroptosis via inducing KAT5/GPX4 in Myocardial infarction. *Front Pharmacol*. 2022;13:906073. doi:10.3389/fphar.2022.906073
28. Li X, Liang J, Qu L, et al. Exploring the role of ferroptosis in the doxorubicin-induced chronic cardiotoxicity using a murine model. *Chem Biol Interact*. 2022:110008. doi:10.1016/j.cbi.2022.110008
29. Fa H-G, Chang W-G, Zhang X-J, Xiao -D-D, Wang J-X. Non-coding RNAs in [illegible]in-induced cardiotoxicity and their potential as biomarkers and therapeutic targets. *Acta Pharmacol Sin*. 2021;42(4):499–507. doi:10.1038/s41401-020-0471-x
30. Marques FZ, Vizi D, Khammy O, Mariani JA, Kaye DM. The transcardiac gradient of cardio-microRNAs in the failing heart. *Eur J Heart Fail*. 2016;18(8):1000–1008. doi:10.1002/ejhf.517
31. Gumus G, Giray D. MicroRNA values in children with rheumatic carditis: a preliminary study. *Rheumatol Int*. 2018;38(7):1199–1205. doi:10.1007/s00296-018-4069-2
32. Gong J, Dou L, Zhou Y. Positive feedback loop of [illegible] SNHG1/miR-16-5p/GATA4 in the regulation of hypoxia/reoxygenation-induced cardiomyocyte injury. *Mol Med Rep*. 2022;25([illegible]).10.3892/mmr.2021.12544
33. Wang X, Shang Y, Dai S, Wu W, Yi [illegible], Cheng L. MicroRNA-16-5p aggravates myocardial infarction injury by targeting the expression of insulin receptor substrates 1 and [illegible]. Myocardial apoptosis and angiogenesis. *Curr Neurovasc Res*. 2020;17(1):11–17. doi:10.2174/1567202617666191223142745
34. Hayasaka T, Takehara N, Arimuma T, et al. Sarcopenia-derived exosomal micro-RNA 16-5p disturbs cardio-repair via a pro-apoptotic mechanism in myocardial infarction in mice. *Sci Rep*. 2021;[illegible](1). doi:10.1038/s41598-021-98761-8
35. Guan JT, Li XX, Peng DW, et al. MicroRNA-18a-5p administration suppresses retinal neovascularization by targeting FGF1 and HIF1A. *Front Pharmacol*. 2020;[illegible]276. doi:10.3389/fphar.2020.00276